Virginia Commonwealth University
VCU Scholars Compass

Physics Publications

Dept. of Physics

2009

Magnetic response of core-shell cobalt ferrite nanoparticles at low temperature

K. Maaz
PINSTECH

M. Usman
Quaid-i-Azam University

S. Karim
PINSTECH

See next page for additional authors

Authors

K. Maaz, M. Usman, S. Karim, A. Mumtaz, S. K. Hasanain, and M. F. Bertino

Magnetic response of core-shell cobalt ferrite nanoparticles at low temperature

K. Maaz,[1,a)] M. Usman,[2] S. Karim,[1] A. Mumtaz,[2] S. K. Hasanain,[2] and M. F. Bertino[3]

[1]*Physics Division, PINSTECH, Post Office Nilore, Islamabad, Pakistan*
[2]*Department of Physics, Quaid-i-Azam University, Islamabad, Pakistan*
[3]*Department of Physics, Virginia Commonwealth University, Richmond, Virginia 23824, USA*

Cobalt ferrite nanoparticles (size: 26 ± 4 nm) have been synthesized by coprecipitation route. The coercivity of nanoparticles follows a simple model of thermal activation of particle moments over the anisotropy barrier in the temperature range of 30–300 K in accordance with *Kneller's law*; however, at low temperatures (<30 K), the coercivity shows some deviation from this law. The saturation magnetization follows the modified Bloch's law in the temperature range of 10–300 K. Exchange bias (H_{ex}) studies of the samples show that H_{ex} increases with decreasing temperature of the sample. A strong increase in the H_{ex} values is found below 30 K for the low applied field (± 20 kOe), while a smaller increase is found for the high applied field (± 90 kOe). The slow increase in the exchange bias at high applied field has been attributed to the high field effects on the surface (shell) spins. These shell spins align along the field direction that weakens the core-shell interface interactions leading to the reduction in the exchange bias at lower temperatures. © *2009 American Institute of Physics*. [DOI: 10.1063/1.3139293]

INTRODUCTION

Cobalt ferrite ($CoFe_2O_4$) is a well-known hard magnetic material with a relatively high coercivity, exchange bias, and moderate magnetization. These properties, along with its chemical and physical stability, make cobalt ferrite very promising candidate for a variety of applications in computer, electronics, and biomedical industries.[1–4] $CoFe_2O_4$ in its bulk form has the inverse spinel structure where Fe^{+2} ions are equally filled in tetrahedral and octahedral sites, while Co^{+2} ions are filled in octahedral sites only. Magnetic properties of $CoFe_2O_4$ depend on the type of the cations and their distribution among the tetrahedral and octahedral sites. It has been observed that the resulting magnetic properties of nanocrystalline $CoFe_2O_4$ are entirely different from its bulk counterpart, which makes this material of great scientific and technological interests.[5–8] The bulk cobalt ferrite has coercivity, saturation magnetization, and Curie's temperature of 900 Oe, 80 emu/g, and 790 K, respectively, which are considerably different from its nanocrystalline form.[9–11] There is a considerable interest in the magnetism and related phenomena in nanoscale $CoFe_2O_4$. The complexity of the situation stems from several competing effects that are sometimes difficult to isolate in these nanoparticles. These include the surface effects, finite size effects, and interparticle interactions. It is now well established that in small size particles, on nanoscale, the surface spins play a dominant role as far as the magnetic properties in these particles are concerned. These spins cause, for example, the reduction in saturation magnetization and enhancement in coercivity with decreasing particle sizes at the nanometric range. Kodama and

Berkowitz[12,13] showed that in ferrite nanoparticles, due to the broken symmetries and exchange bonds at the surfaces, the spins at the surface of ferrite nanoparticles do not follow the core anisotropy direction and become disordered or may become canted leading to even high anisotropy compared to the core of the nanoparticles. Such particles are generally termed as the *core-shell* nanoparticles, where the core spins behave like ferromagnetic (FM) or ferrimagnetic (FI), and the shell is composed of disordered spins or canted spins. The core-shell picture is not only limited to the ferrite nanoparticles, this also includes other configurations such as CoO, FeO, and other complex oxides as well.

In this work, we report low temperature magnetic properties of 26 ± 4 nm cobalt ferrite nanoparticles and the results are explained with reference to the disordered surface spins, finite size effects, and thermal activation model. This has not been reported in detail previously, to the best of our knowledge. One of the interesting phenomena observed by the core-shell nanoparticles is the exchange bias effect, i.e., when the particles are cooled in the presence of some magnetic field, the resultant hysteresis loop appears shifted (asymmetric) along both the field and magnetization axes. The appearance of the shifted hysteresis loop is generally attributed to the core-shell nature of the nanoparticles. Here the exchange bias for these nanoparticles has also been investigated from room temperature (300 K) to 10 K and the results have been explained with reference to the core-shell structure in these nanoparticles.

EXPERIMENTAL

The samples reported in this study were synthesized by coprecipitation technique that has been described in detail elsewhere.[14,15] The starting materials were iron chloride, cobalt chloride, and nickel chloride, while the oleic acid was

---

a)Author to whom correspondence should be addressed. Electronic addresses: maaz@impcas.ac.cn and maaz@phys.qau.edu.pk. Tel.: +92-321-5029820. FAX: +92-51-9290275.
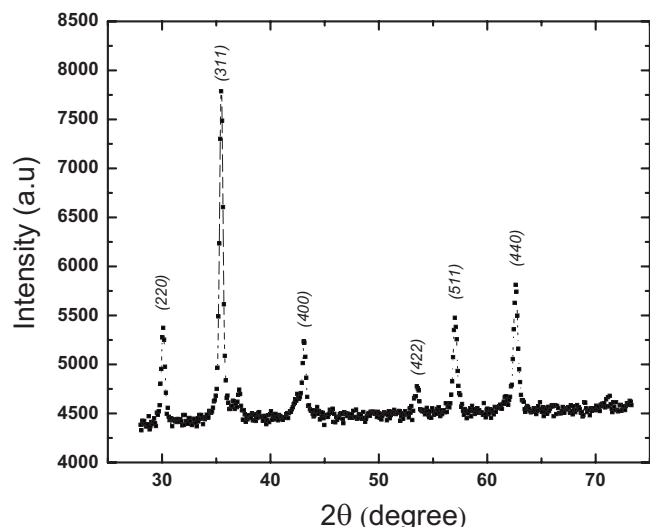
105, 113917-1

FIG. 1. XRD pattern of $CoFe_2O_4$ nanoparticles prepared by coprecipitation method after annealing at 600 °C with average crystallite size of about 26 ± 4 nm.

FIG. 2. High resolution TEM of $CoFe_2O_4$ nanoparticles. The inset in the figure shows the SAED analysis of the sample.

used as the surfactant. The reaction was carried out at 80 °C and double distilled de-ionized water was used as the solvent to minimize the impurities in the final product. After completion of the reaction, the solution was cooled to room temperature and then centrifuged in order to isolate the supernatants. The final product was dried at 100 °C overnight and then annealed at 600 °C to get the desired particles. The size and size distribution were controlled by controlling the relative nucleation and growth rates during the reaction. Smaller and uniformly distributed particles were obtained if the nucleation rate was higher than the growth rate. Large pH values in the range of 12–13 were used in accordance with the prediction that higher production yields are expected for larger pH values.[14]

The physical characterization of the nanoparticles was performed by x-ray diffractometer (XRD-7000, Shimadzu, Cu $K\alpha$=0.154 178 nm) and transmission electron microscope (TEM, JEM-3010, JEOL). For the magnetic characterization of the sample, the powdered sample was mixed in a nanomagnetic epoxy raisin and was dried in a cylindrical mold (height of 4 mm and diameter of 2 mm). The dc magnetic measurements were performed by quantum design physical property measurement system.

RESULTS AND DISCUSSION

The x-ray diffraction (XRD) pattern of cobalt ferrite nanoparticles is shown in Fig. 1. All the peaks in the pattern correspond to the expected inverse spinel structure of $CoFe_2O_4$. These peaks are indexed to the cubic $CoFe_2O_4$ phase according to Ref. 16. The particle size has been calculated from the XRD line broadening of the (311) peak using Scherrer's equation.[17] Figure 2 shows the transmission electron microscopy image of the prepared nanoparticles. In the transmission electron microscopy (TEM) analysis we see that most of the particles appear spherical in shape, separated from each other; however, some agglomerated particles are also present in the sample that appear like a single big particle in the image. The inset in Fig. 2 shows the selected area
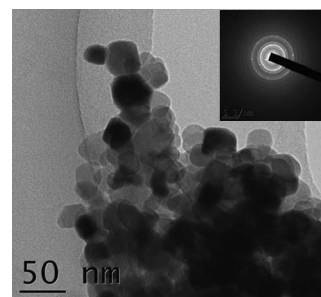
electron diffraction (SAED) pattern of the sample that represents the well crystalline nature of the prepared nanoparticles. It is to be noted that the size of the nanoparticles as calculated from the XRD pattern has been found in good matching with TEM visual results.

The magnetization measurements were made at different temperatures, starting from room temperature (300 K) down to 10 K. In Fig. 3 we have presented $M(H)$ loops at different temperatures of 10, 50, 100, 150, 200, 250, and 300 K for the applied fields of up to 90 kOe. The inset in the figure shows the expanded region around the origin (in the field region of ± 2 kOe) in order to make the coercivity more visible at various temperatures. One of the remarkable features in the $M(H)$ loops is that the magnetization does not saturate, especially at low temperatures, even at high applied field of 90 kOe (see Fig. 3). This is generally attributed to the canted or disordered spins at the surface of the nanoparticles that are difficult to align along the field direction, causing an unsaturated magnetization in these nanoparticles at low temperatures. The coercivity values at different temperatures, as calculated from the $M(H)$ loops, are plotted in Fig. 4. We observed a monotonic increase in coercivity with decreasing temperature of the nanoparticles. The reason for the increasing coercivity with decreasing temperature can be under-
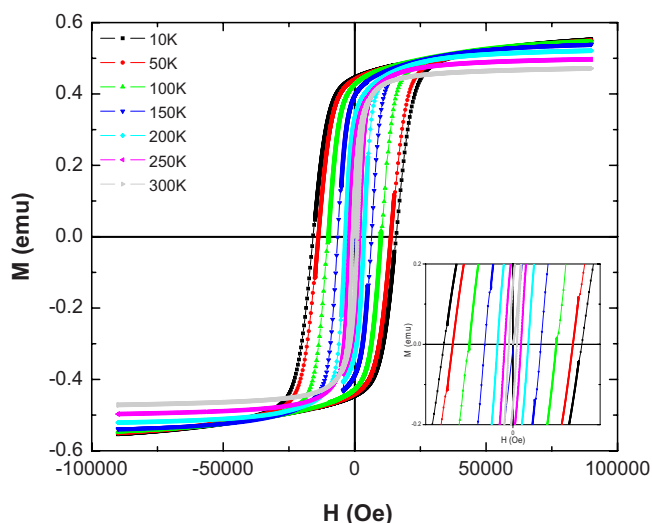

FIG. 3. (Color online) $M(H)$ loops of $CoFe_2O_4$ nanoparticles taken at 10, 50, 100, 150, 200, 250, and 300 K up to maximum field of ± 90 kOe. The inset in the figure shows the expanded region around the origin in order to make the coercivity visible at various temperatures.
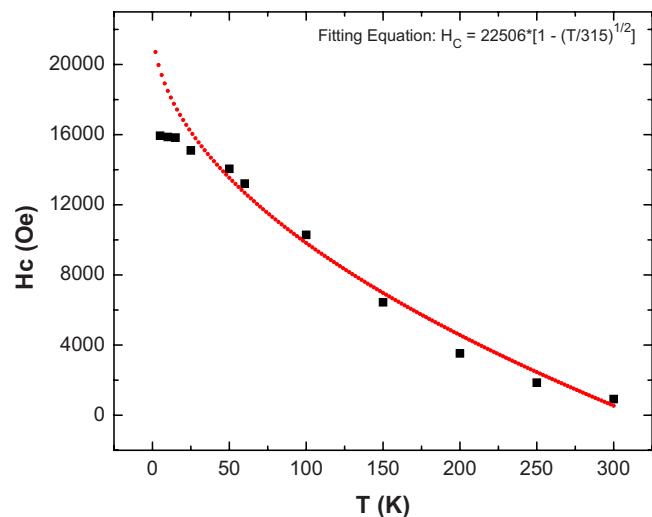
FIG. 4. (Color online) Temperature dependence of coercivity for $CoFe_2O_4$ nanoparticles. The curve shows the fit according to *Kneller's law* ($H_C = H_{C0}[1-(T/T_B)^{1/2}]$) for our system.

FIG. 5. (Color online) Saturation magnetization (M_S) as a function of temperature for $CoFe_2O_4$ nanoparticles. The line is the fit curve according to modified Bloch's law for saturation magnetization of FM materials.

stood by considering the effects of thermal fluctuations of the blocked moment, across the anisotropy barrier. For an assembly of noninteracting three-dimensional single domain magnetic nanoparticles with uniaxial anisotropy, the coercivity (H_C) in the temperature range ($0-T_B$) can be written in the form of simple model of thermal activation of particle moments over the anisotropy barriers (Kneller's law) as[18,19]

$$H_C = H_{C_0}\left(1 - \frac{T}{T_B}\right)^{1/2},$$

where, H_{C_0} is the coercivity at $T=0$ K and can be estimated by extrapolating the H_C versus temperature curve toward the field axis, while T_B is the superparamagnetic blocking temperature of the nanoparticles. Referring to Fig. 4, the red line shows the fit curve according to the above relation (Kneller's law) using the blocking temperature as the fitting parameter. As evident from the figure, the data fit well to the above relation in the high temperature region (300–30 K). The coercivity at $T=0$ K ($H_{0\ K}$) for these nanoparticles, as determined from the fit, is ∼22.5 kOe, while the blocking temperature is ∼315 K. Previously we have reported the coercivity and blocking temperature (T_B) for the same sample to be ∼16 kOe and ∼268 K.[14] The T_B value found here (315 K) is larger than the value reported in Ref. 14. The difference between the two values arises due to the fact that in our previous work the data were taken under a cooling field of 5 kOe that usually shifts the peak to the lower values in the $M(T)$ curves. We see that Kneller's relation fits very well in the temperature range of (300–30 K); however, the experimental data deviate from this law (fit curve) below ∼30 K. Thus the simple model of thermal activation of particle moments over the anisotropy barriers does not appear to be applicable below 30 K in this case. The deviation of H_C from the thermal activation model at low temperatures can be explained in the way that for $CoFe_2O_4$ nanoparticles the surface spins (shell spins) freeze in their random sates, giving no further response to the applied field that resultantly prevent the core spins to further align along the field direc-
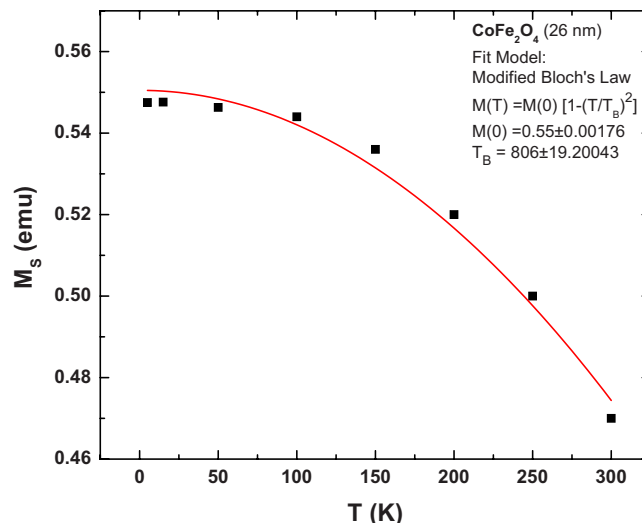
tion. This, in turn, saturates the coercive fields at low temperatures (below 30 K). Our results are in agreement with the work of Iglesias and Labarta[20] based on the Monte Carlo simulation of the dependence of coercivity on temperature of γ-Fe_3O_4 spherical nanoparticles.

The magnetization measurements at different temperatures for cobalt ferrite nanoparticles are presented in Fig. 5. From the figure, it is evident that the saturation magnetization (M_S) increases with decreasing temperature of the sample. For a bulk FM/MI system, the saturation magnetization below the Curie temperature of the system follows Bloch's law of the form $[M(T) = M(0)[1-(T/T_0)^{\alpha}]$.[21] Where $(1/T_0)^{\alpha}$ is called the Bloch constant (B) and it depends on the structure of the material. $M(T)$ is the temperature-dependent magnetization and α is Bloch's exponent with a value of $3/2$ for bulk materials. This law is generally valid for bulk material in the high temperature range. However, at the nanoscale, due the finite size effects, the thermal dependence of magnetization deviates from Bloch's law as the magnons with wavelength larger than the particle dimensions cannot be excited and a threshold of thermal energy is required to generate spin waves in these small scaled particles. Thus for nanoparticles, the spin-wave structure is modified in the form of a power law (T^{α}) with Bloch's exponent larger than its bulk value of $3/2$. This is known as the modified Bloch's law.[22,23] The value of α in the modified Bloch's law has been experimentally determined by Auino *et al.*[23] They found that for large sized $CuFe_2O_4$ nanoparticles, the value of α was $3/2$, whereas for smaller particles, this value was close to 2. The difference was attributed to finite size effects in smaller particles. Now referring back to our system of $CoFe_2O_4$ nanoparticles (see Fig. 5) we see that the modified Bloch's law with $\alpha=2$ (shown by the red line) is satisfied for these particles in the full temperature range of 10–300 K. Thus the modified spin-wave spectrum is applicable to $CoFe_2O_4$ nanoparticles.

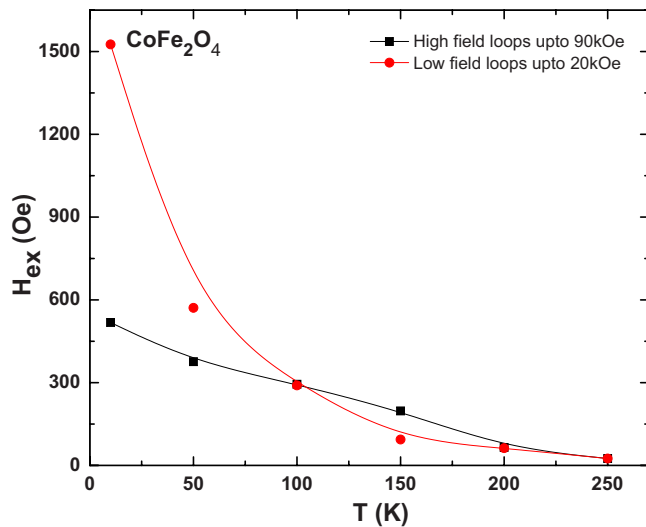We now turn to the exchange bias effects in cobalt ferrite nanoparticles. Figure 6 shows the dependence of exchange

FIG. 6. (Color online) The dependence of exchange field (H_{ex}) on temperature for $CoFe_2O_4$ sample measured at different applied fields (20 and 90 kOe). The pronounced increase in H_{ex} values at 20 kOe is evident at low temperatures.

field (H_{ex}) on temperature on the basis of two different applied fields. In the first case the loop was recorded under ± 90 kOe (shown by the black line in the figure), while in the second case $M(H)$ loops were obtained under a field of ± 20 kOe (shown by the red line in the figure). In both cases the cooling field was 4 kOe. It is evident from the figure that the samples exposed to 20 kOe show more exchange bias as compared to those exposed to 90 kOe for the same cooling field. Furthermore, it was found that the exchange bias in both cases increases with decreasing temperature of the sample. In Fig. 6 we see the dependence of H_{ex} on temperature of the sample that was observed to be stronger in the case of 20 kOe as compared to 90 kOe especially at low temperatures. A sharp rise in H_{ex} was observed at low temperatures like it was observed and discussed in the case of coercivity versus temperature curve (see Fig. 4) for the same sample. Because of the exchange coupling between the surface and the core spins, the field cooling can select a surface spin configuration which favors the particle being magnetized in the field cooling direction resulting in large coercivities and large exchange bias values. To explore the temperature dependence of exchange bias for our nanoparticles in detail, we refer to Fig. 6 where we see a sharp decrease in H_{ex} with increasing temperature, starting from lower temperature side, and then the decrease is lower in the high temperature range of 50–250 K, while it vanishes beyond 250 K. The decrease in H_{ex} with increasing temperature may be explained on the basis of the core-shell model in cobalt ferrite nanoparticles. The frozen disordered spin structure at low temperature (10 K) starts unfreezing with increasing temperature of the sample, thereby decreasing the surface anisotropy that is responsible for the exchange bias effects in these nanoparticles. Therefore the exchange bias decreases with increasing temperature of the sample. It has been reported in literature that the exchange bias generally disappears at a temperature below the blocking temperature of the FM/FI core[24] and that is ~ 315 K for our nanoparticles as

discussed earlier; we see that the value of H_{ex} is negligible even well below T_B. The large H_{ex} values at lower temperatures could also be due to the pronounced growth of magnetic anisotropy of the core and shell in $CoFe_2O_4$ nanoparticles. This growth of anisotropy resultantly increases the core-shell (spin) interaction that, in turn, increases the H_{ex} values at the lower temperatures.

When we are dealing with nanoparticles at low temperatures, the anisotropy may be a huge function of temperature. Thus other factors, apart from the enhancement of anisotropy, such as the structural properties that are intrinsic to the nanoparticles, including volume distribution, randomness of anisotropy axes, and interparticle interactions may also influence the thermal dependence of exchange bias and coercivity in nanoparticles.[25] It is interesting to note that the exchange bias values are lower for the loops exposed to higher fields (± 90 kOe) as compared to those taken at lower fields (± 20 kOe). We attribute this to the high field effects where most of the surface spins turn along the field direction resulting in the reduction in the core-shell interface interaction and hence the exchange bias in core-shell cobalt ferrite nanoparticles.

CONCLUSION

Coercivity and saturation magnetization of 26 ± 4 nm $CoFe_2O_4$ nanoparticles showed an increasing behavior with decreasing temperature. The enhanced coercivity at lower temperatures has been attributed to the increasing effects of thermal fluctuations of the blocked moments across the anisotropy barriers according to Kneller's law. The saturation magnetization of the nanoparticles followed the modified Bloch's law based on the modified spin- wave spectrum for nanoparticles due to their finite size effects. The exchange fields were found to increase with decreasing temperature of the sample in the range of 10–300 K. A sharp increase in the exchange bias values was found for the low applied fields, while a relatively low increase was found for the higher applied fields. This has been attributed to the high field effects where most of the surface spins turn along the field direction, leading to the weaker core-shell interface interactions that decreases the exchange bias effects in these nanoparticles.

ACKNOWLEDGMENTS

[1]P. Tartaj, M. D. Morales, and V. V. Sabino, J. Phys. D **36**, R182 (2003).
[2]S. D. Bader, Rev. Mod. Phys. **78**, 1 (2006).
[3]C. A. Ross, Annu. Rev. Mater. Res. **31**, 203 (2001).
[4]R. W. Wood, J. Miles, and T. Olson, IEEE Trans. Magn. **38**, 1711 (2002).
[5]C. J. Brumlik and C. R. Martin, Anal. Chem. **59**, 2625 (1992).
[6]Z. Cai and C. R. Martin, J. Am. Chem. Soc. **111**, 4138 (1989).
[7]S. K. Chakarvarti and J. Vetter, Nucl. Instrum. Methods Phys. Res. B **62**, 109 (1991).

[8]S. K. Chakarvarti and J. Vetter, J. Micromech. Microeng. **3**, 57 (1993); Radiat. Meas. **29**, 149 (1998).

[9]D. J. Craik, *Magnetic Oxides* (Wiley, London, 1975), pt. 2, p. 703.

[10]L. D. Tung, V. Kolesnichenko, D. Caruntu, N. H. Chou, C. J. O'Connor, and L. Spinu, J. Appl. Phys. **93**, 7486 (2003).

[11]S. T. Alone and K. M. Jadhav, Pramana, J. Phys. **70**, 173 (2008).

[12]R. H. Kodama and A. E. Berkowitz, J. Appl. Phys. **81**, 5552 (1997).

[13]R. H. Kodama and A. E. Berkowitz, Phys. Rev. Lett. **77**, 394 (1996).

[14]K. Maaz, A. Mumtaz, S. K. Hasanain, and A. Ceylan, J. Magn. Magn. Mater. **308**, 289 (2007).

[15]K. Maaz, S. Karim, A. Mumtaz, S. K. Hasanain, J. Liu, and J. L. Duan, J. Magn. Magn. Mater. **321**, 1838 (2009).

[16]JCPDS Card No. 791744.

[17]T. Fukui, C. Sakurai, and M. Okuyama, J. Mater. Res. **7**, 791 (1992).

[18]E. F. Kneller and F. E. Luborsky, J. Appl. Phys. **34**, 656 (1963).

[19]X. Batlle, M. Garcia del Muro, J. Tejada, H. Pfeiffer, P. Goand, and E. Sinn, J. Appl. Phys. **74**, 3333 (1993).

[20]O. Iglesias and A. Labarta, Phys. Rev. B **63**, 184416 (2001).

[21]F. Bloch, Z. Phys. **61**, 206 (1931).

[22]K. Mandal, S. Mitra, and P. Anil Kumar, Europhys. Lett. **75**, 618 (2006).

[23]A. Auino, M. H. Sousa, H. R. Rechenbrg, G. F. Goya, F. A. Tourinho, and J. Depeyrot, J. Metastable Nanocryst. Mater. **20–21**, 694 (2004).

[24]F. Radu, M. Etzkorn, R. Schmitte, K. Westerholt, and H. Zabel, Phys. Rev. B **67**, 134409 (2003).

[25]O. Iglesias, A. Labarta, and X. Batlle, J. Nanosci. Nanotechnol. **8**, 2761 (2008).